Supporting Information for

Synergistic Surface Modulation with Isotropic 2D GA_2PbI_4 and Lewis Base Enhances Efficiency and Stability of Perovskite Solar Cells

Peiquan Song,‡[a] Lina Shen,‡[a] Lingfang Zheng,[a] Enlong Hou,[a] Peng Xu,[a] Jinxin Yang,[a] Chengbo Tian,[a] Zhanhua Wei,*[a] Xiaguang Zhang,*[b] and Liqiang Xie*[a]

[a]Xiamen Key Laboratory of Optoelectronic Materials and Advanced Manufacturing, Institute of Luminescent Materials and Information Displays, College of Materials Science and Engineering, Huaqiao University, Xiamen, 361021, China
E-mail: lqxie@hqu.edu.cn, weizhanhua@hqu.edu.cn

[b]Key Laboratory of Green Chemical Media and Reactions, Ministry of Education, Collaborative Innovation Center of Henan Province for Green Manufacturing of Fine Chemicals, College of Chemistry and Chemical Engineering, Henan Normal University, Xinxiang, 453007, China
E-mail:zhangxiaguang@htu.edu.cn

‡ Authors with equal contributions.

Materials

Methylammonium iodide (MAI), methylammonium bromide (MABr), and formamidinium iodide (FAI) were bought from Greatcell Solar. Lead iodide (PbI_2, 99.99%) and guanidinium iodide (GAI, >97%) were purchased from TCI. Methylamine hydrochloride (MACl) was obtained from Xi'an Polymer Light Technology Corporation. 2,2',7,7'-tetrakis[N,N-di(4-methoxyphenyl)amino]-9,9-spirobifluorene (Spiro-OMeTAD, 99%) were bought from Shenzhen Feiming Technology Corporation. [(2,6-(4,8-bis(5-(2-ethylhexyl)thiophene-2-yl)-benzo[1,2-b:4,5-b′]dithiophene))-alt-(5,5-(1′,3′-di-2-thienyl-5′,7′-bis(2-ethylhexyl)benzo[1′,2′-c:4′,5′-c′]dithiophene-4,8-dione)] (PBDB-T, 99%) was purchased from Solarmer. Hydrochloric acid (HCl) was purchased from Shanghai Hushi Corporation. Guanidinium acetate (GAAc, 99%), formamidinium acetate (FAAc, 99%), urea, thioglycolic acid (TGA, 98%), $SnCl_2 \cdot 2H_2O$ (>99.995%), N, N-dimethylformamide (DMF, anhydrous, 99.8%), dimethyl sulfoxide (DMSO, anhydrous, 99.9%), isopropanol (IPA, anhydrous, 99%), chlorobenzene (CB, 99.8%), acetonitrile (anhydrous, 99.8%), bis(trifluoromethane) sulfonimide lithium salt (99.95%) and 4-tert-butylpyridine (TBP, 96%) were obtained from Sigma-Aldrich.

Device Fabrication:

Electron transport layer deposition: First, FTO glass substrates were cleaned by sequential ultrasonic treatment in detergent, deionized water, acetone, isopropyl alcohol, and ethanol. The cleaned substrates were then treated for 15 minutes with O_2 plasma. The chemical bath deposition (CBD) solution was prepared by mixing 1250 mg of urea, 1250 μL of HCl, 25 μL of TGA, and 275 mg of $SnCl_2 \cdot 2H_2O$ into 100 mL of deionized water. The FTO substrates and the CBD solution were loaded onto a glass reaction vessel and reacted at 97 °C for 5 hours. Then, the FTO substrates were taken out from the CBD solution, rinsed with deionized water, and subjected to ultrasonication in IPA for 5 minutes. Finally, it was annealed on a hotplate at 170°C for 1 hour.

Perovskite absorber deposition: On the CBD SnO_2 layer, 1.5 M PbI_2 with 5% CsI (dissolved in DMF/DMSO=9/1, v/v) was spin-coated at 2,500 rpm for 30 s and annealed at 70 °C for 1 minute in an N_2-filled glove box. Then, a solution of organic salts (120 mg of FAI, 20 mg of MAI, 3 mg of MABr, and 5 mg of MACl dissolved in 2 mL of IPA) was spin-coated at 1,500 rpm for 30 s and then annealed at 150 °C for 15 minutes in the ambient air (30% relative humidity). After cooling down to room temperature, GAAc with a concentration of 2 mg mL^{-1} in IPA was spin-coated at 4,000 rpm for 30 s. Subsequently, the sample was heated on a hotplate at 100°C for 10 minutes.

Hole transport layer (HTL) and metal electrode deposition: The HTL solution consists of 72.3 mg of Spiro-OMeTAD, 17.5 μL of lithium bis(trifluoromethane) sulfonamide salt (520 mg dmL^{-1} in acetonitrile), and 28.8 μL of 4-tertbutylpyridine in 1 mL of chlorobenzene. The prepared HTL solution was spin-coated on the perovskite films at 4,000 rpm for 30 s. For the thermal stability test, the Spiro-OMeTAD solution was mixed with PBDB-T solution (5mg mL^{-1} dissolved in chlorobenzene) at a volume ratio of 4: 1. Finally, A 80 nm Ag was deposited via thermal evaporation to complete the solar cell device.

Characterization

Photovoltaic characteristics were measured using a Keithley 2400 source meter under simulated AM1.5G irradiation under an Xe lamp simulator (Enli SS-F5). The light intensity was calibrated to 1 sun illumination using a NERL-calibrated silicon photodiode with a KG5 filter. The *J-V* curves of all devices were tested at a scan rate of 40 mV s^{-1} with an aperture mask (0.12 cm^2). The reverse scan was from V_{OC} to J_{SC} (1.25 V to 0 V), and the forward scan was from J_{SC} to V_{OC} (0 V to 1.25 V).^{13}C NMR spectra were measured using a Bruker Avance III 500 MHz NMR spectrometer. UV-Vis absorption, photoluminescence, and electroluminescent spectra were collected on OceanInsight Spectrometer. Time-resolved photoluminescence and temperature-dependent photoluminescence measurements were carried out using the FLS1000 (Edinburgh Instrument, UK). X-ray diffraction (XRD) patterns were taken with Cu K_α radiation on a Rigku-SmartLab X-ray diffraction instrument. Grazing-incidence wide-angle X-ray scattering (GIWAXS) patterns were acquired at the XEUSS WAXS/SAXS system (Xenocs, France). X-ray photoelectron spectroscopy data were obtained from the Thermo Scientific K-Alpha+. An Al K_α (1486.7 eV) source gun with 400 μm X-ray spot was used. The pass energy was 30 eV and the energy step was 0.05 eV. Ultraviolet photoelectron spectroscopy (UPS) measurements were carried out on a Thermo-Fisher ESCALab Xi+ system at a bias of -5 V using a He-I_α (21.22 eV) UV light source. PL mapping was performed on Leica TCS SP8 Confocal laser scanning microscopy. The excitation wavelength was 488 nm, the detection wavelength range was 790-800 nm, and the fluorescence signal was probed by a PMT detector with a gain value constant at 400. Scanning electron microscope (SEM) images were obtained from a JEOL-JSM-7610F-plus field-emission scanning electron microscopy. The transient photovoltage (TPV) measurement transient time is 1 μs,potentiostat setting time is 0.2 μs,and the mode of light intensity course is on-off. TPV, Mott-Schottky polt is obtained by Capacitance-voltage test from 0→1.2 V under 10 KHz, and admittance spectroscopy analysis acquired by Capacitance-frequency from 1MHz→1Hz. TPV, Capacitance-voltage, Capacitance-frequency

measurements were carried out on a Zahner electrochemical workstation. The admittance spectroscopy analysis The conductivity of the perovskite films at different temperatures was measured by CHI-660e electrochemical workstation. Operational stability data was tracked on a solar cell stability test system by Suchow DeRui Corporation.

Supplementary Note 1: Calculation of the trap density (N_t).

The N_t can be calculated using Capacitance-frequency and Capacitance-voltage measured in the dark state, and estimated by a formula: $N_t(E_\omega) = -\frac{\omega}{K_B T} \times \frac{V_{bi}}{eW} \times \frac{dC}{d\omega}$. Where ω is the angular frequency of the ac signal, K_B is Boltzmann constant, T is temperature, $K_B T = 0.026$ eV in room temperature; V_{bi} is the built-in voltage in the heterojunction, W is the width of the depletion layer; C is capacitance. A Mott-Schottky plot: $\frac{A^2}{C^2} = \frac{2(V_{b_i} - V)}{q\varepsilon\varepsilon_0 N}$ describes a straight line where the intersection on the bias axis determines V_{bi} and the slope gives the impurity doping density N. The depletion layer width W can be calculated by $W = \sqrt{\frac{2\varepsilon\varepsilon_0 V_{bi}}{qN}}$.The energy $E\omega$ can be estimated by the formula $E_\omega = K_B T \times In\frac{2\beta_\rho N_v}{\omega}$. Where β_ρ is capture coefficient of hole, N_v is the effective density of states in the valence band. The β_ρ is 10^{-8} cm^3/s, and the N_v is $2.524\times10^{19}/cm^3$ for the perovskite film based $FAPbI_3$.[1, 2]

DFT calculations

To calculate the adsorption energy, the periodic structures were calculated in the Vienna ab initio simulation package (VASP) using the Perdew-Burke-Ernzerhof function with the generalized gradient approximation.[3] The DFT-D3 method was employed to correct the Van der Waals interactions of the system. The spin polarization calculation was carried out in the geometric optimization. The plane-wave basis cutoff was set as 450 eV, the energy criterion was set as 10^{-5} eV, and the force criterion was set as 0.02 eV/Å. The adsorption structure was studied by using a three-layer (2 × 2) perovskite supercell and a 15 Å vacuum layer. The bottom layer of perovskite was fixed. A 3 × 3 × 1 Monkhorst-Pack k-point sampling grid was used to optimize the geometrical structure.

The binding energies were calculated by the following equation:

$E=E_{tot}-E_{substrate}-E_{mole}$,

where E_{tot}, $E_{substrate}$, and E_{mole} are the total electronic energies of the total system, the perovskite substrate, and the ion, respectively. The structure of them was based on the optimized structure of the system.

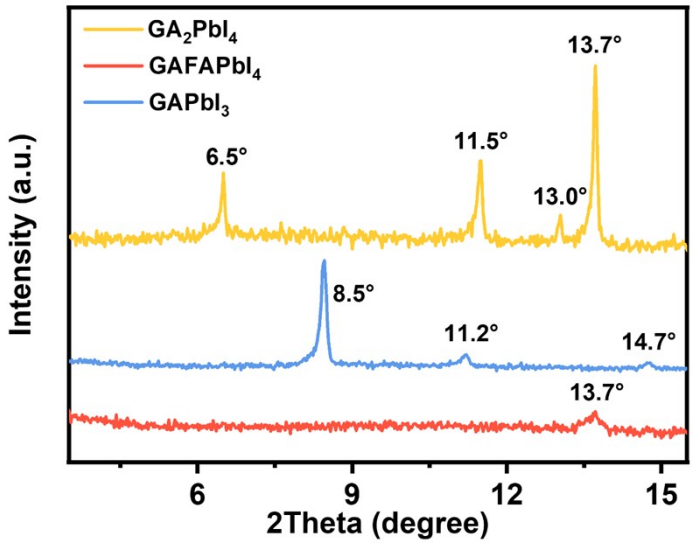

Fig. S1 XRD patterns of the GA_2PbI_4, $GAFAPbI_4$, and $GAPbI_3$ perovskite films.

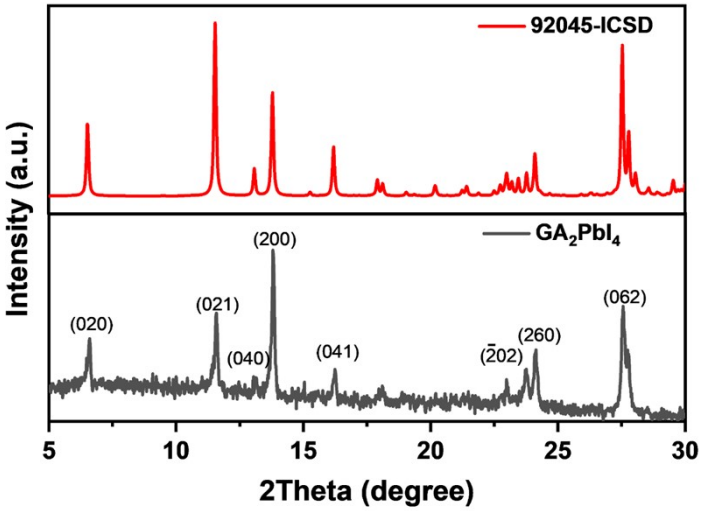

Fig. S2 XRD patterns of the 2D GA_2PbI_4 films and the single crystal ICSD card.[4]

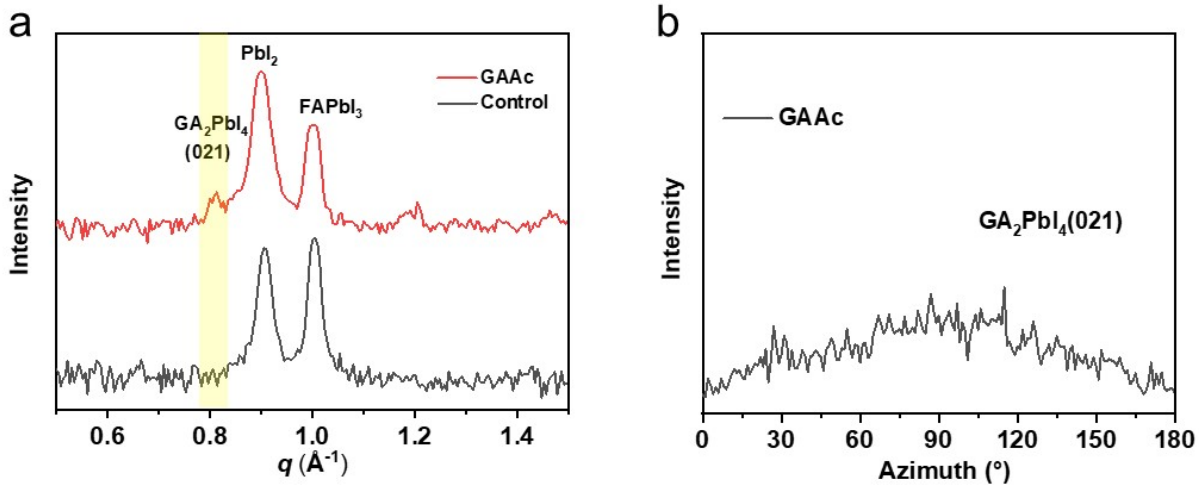

Fig. S3 (a) GIWAXS profile of the control and GAAc-treated perovskite films. (b) The azimuthal integration profile of the (021) diffraction of GA_2PbI_4 from the GIWAXS pattern.

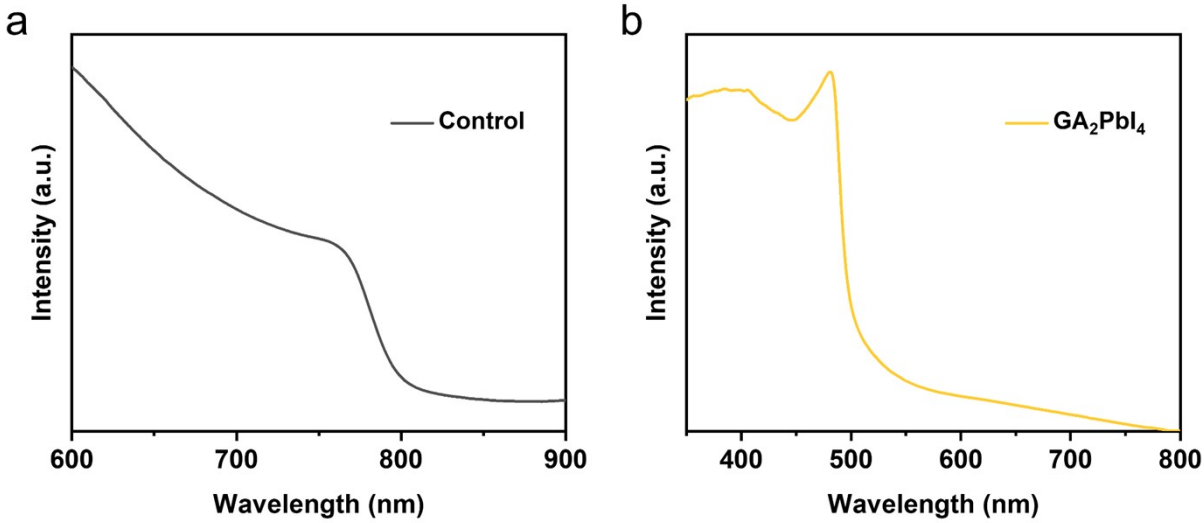

Fig. S4 UV-vis absorption spectrum of spin-coated (a) Control and (b) GA_2PbI_4 perovskite film on the glass substrate.

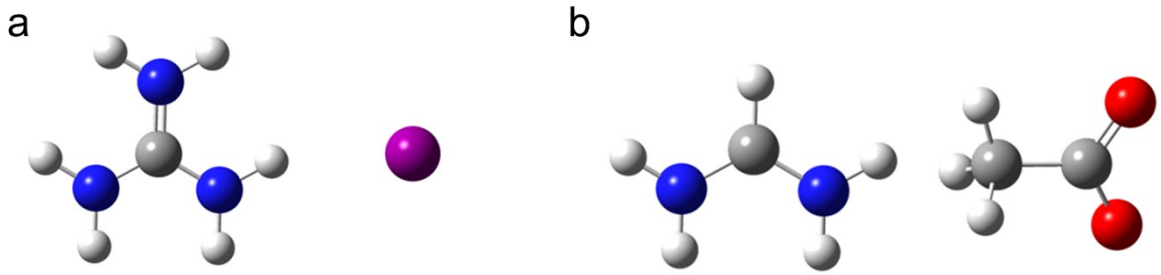

Fig. S5 Molecular structure of (a) GAI and (b) FAAc.

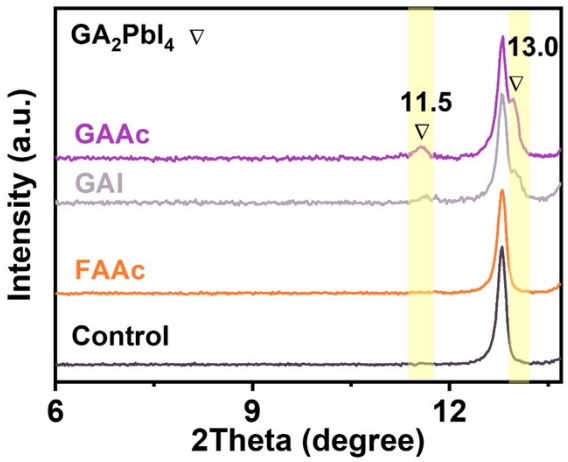

Fig. S6 XRD patterns of the control, GAI, FAAc, and GAAc-treated perovskite films.

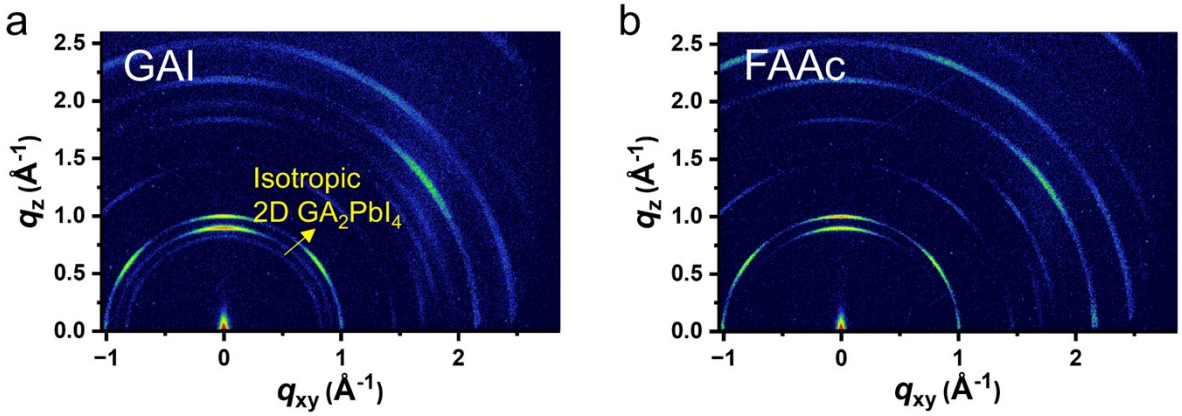

Fig. S7 GIWAXS patterns of (a) GAI and (b) FAAc-teated perovskite films.

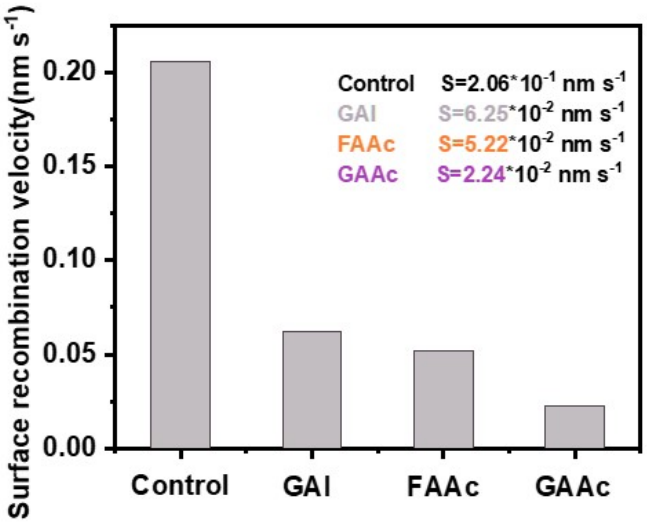

Fig. S8 Surface recombination velocity of the control, GAI, FAAc, and GAAc treated perovskite films.

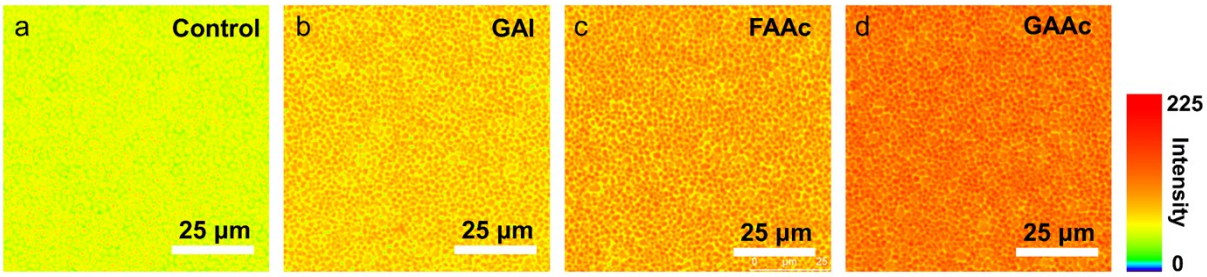

Fig. S9 PL-Mapping images of the (a) control, (b) GAI, (c) FAAc, and (d) GAAc treated perovskite films.

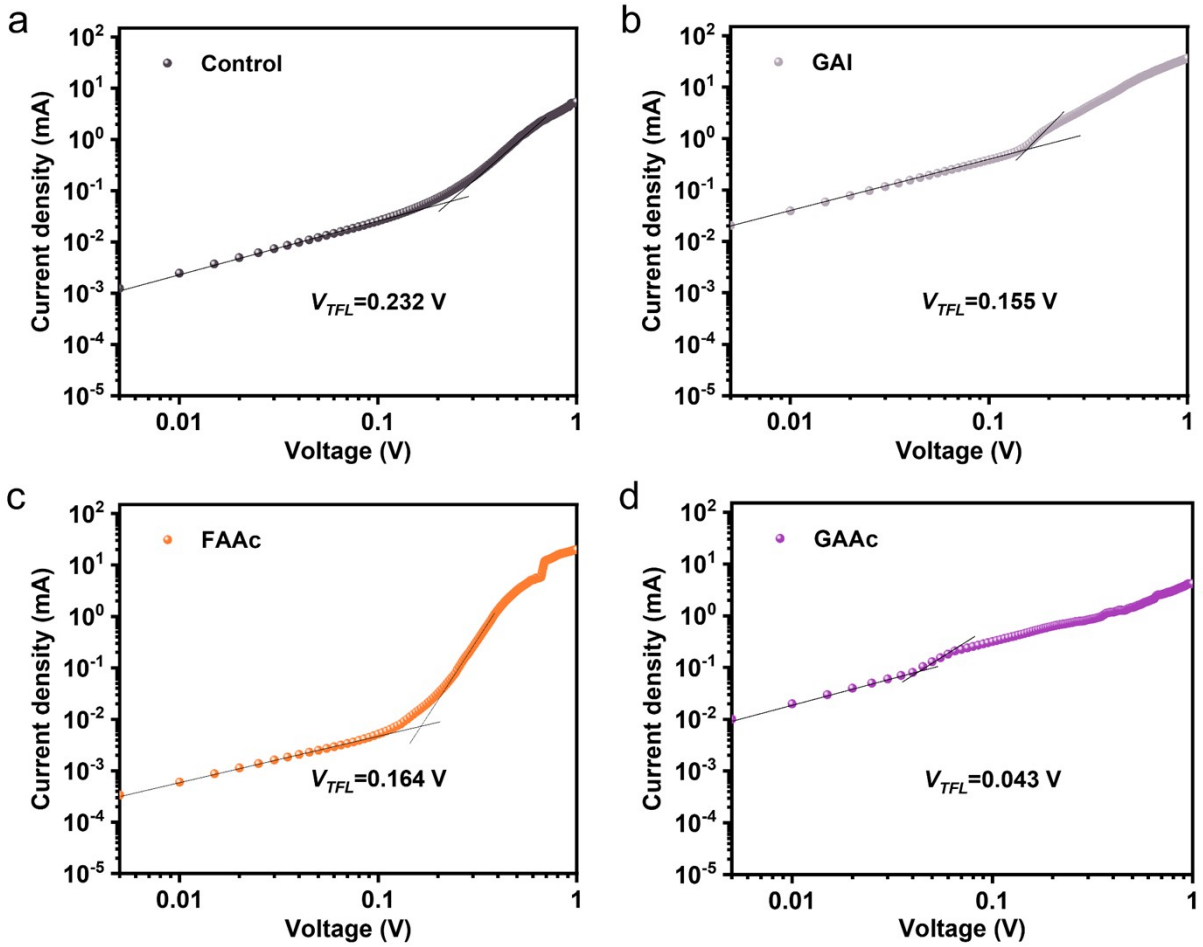

Fig. S10 SCLC measurements of the electron-only device with the device architecture of ITO/SnO_2/perovskite/PCBM/Ag based on the (a) control, (b) GAI, (c) FAAc, and (d) GAAc treated perovksites.

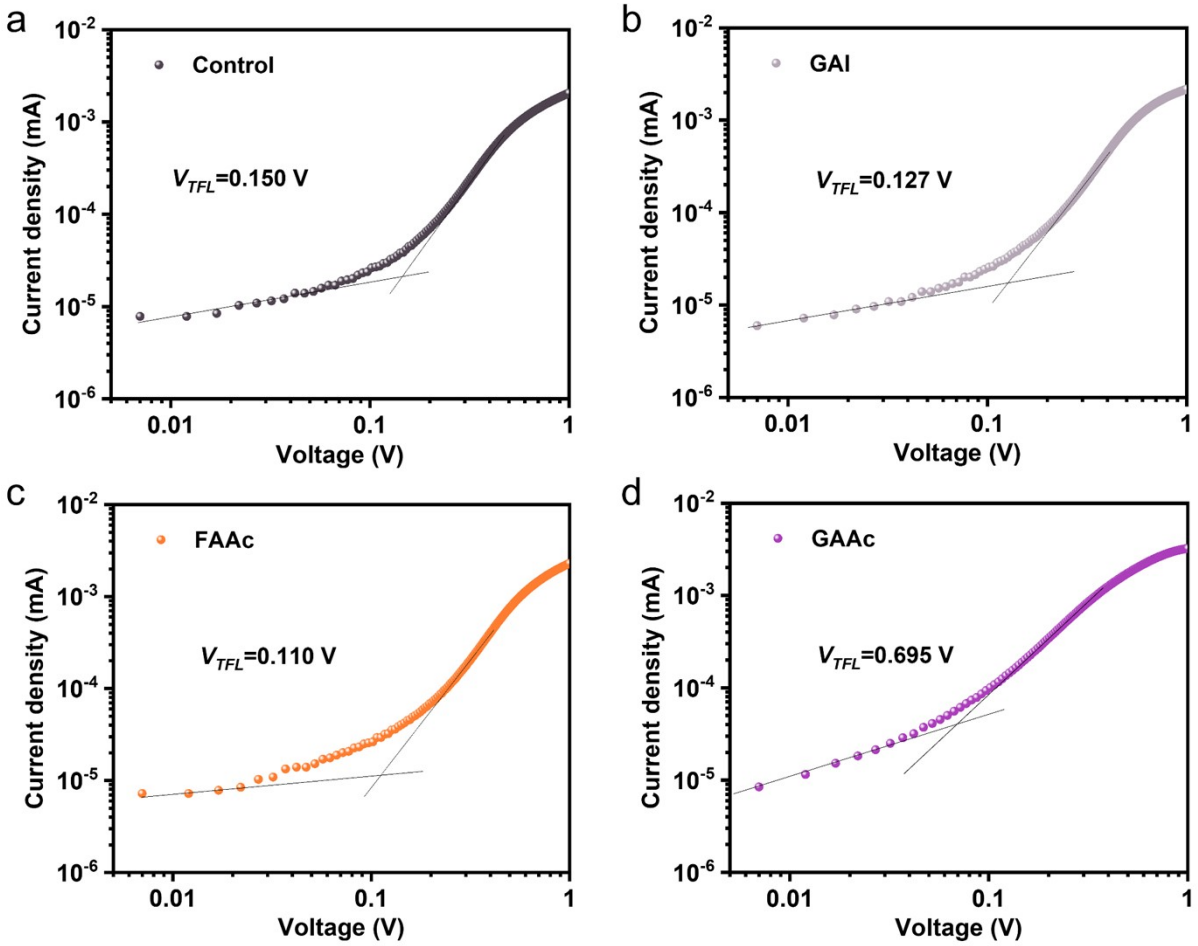

Fig. S11 SCLC measurements of the hole-only devices with the architecture of ITO/PEDOT:PSS/perovskite/PTAA/Ag based on the (a) control, (b) GAI, (c) FAAc, and (d) GAAc treated perovksites.

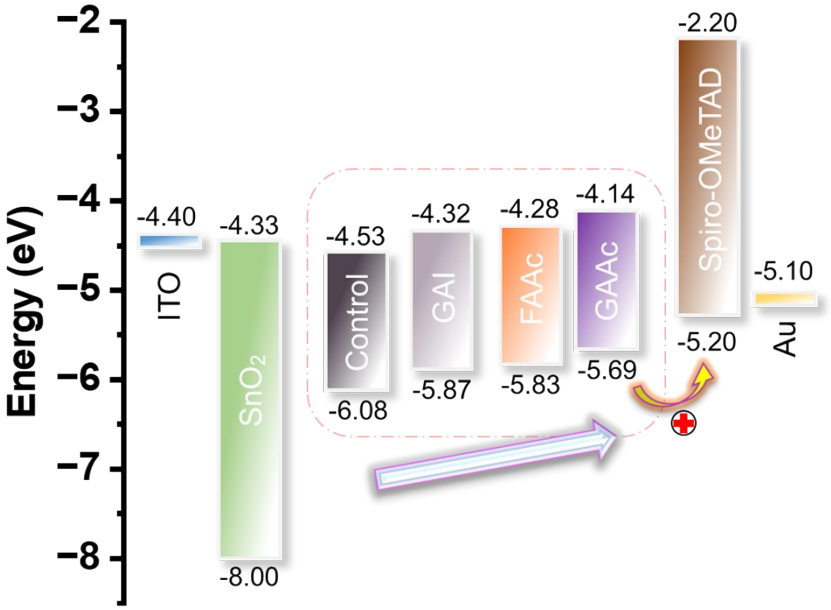

Fig. S12 Energy band diagram of solar cell devices based on the control, GAI, FAAc, and GAAc treated perovksites.

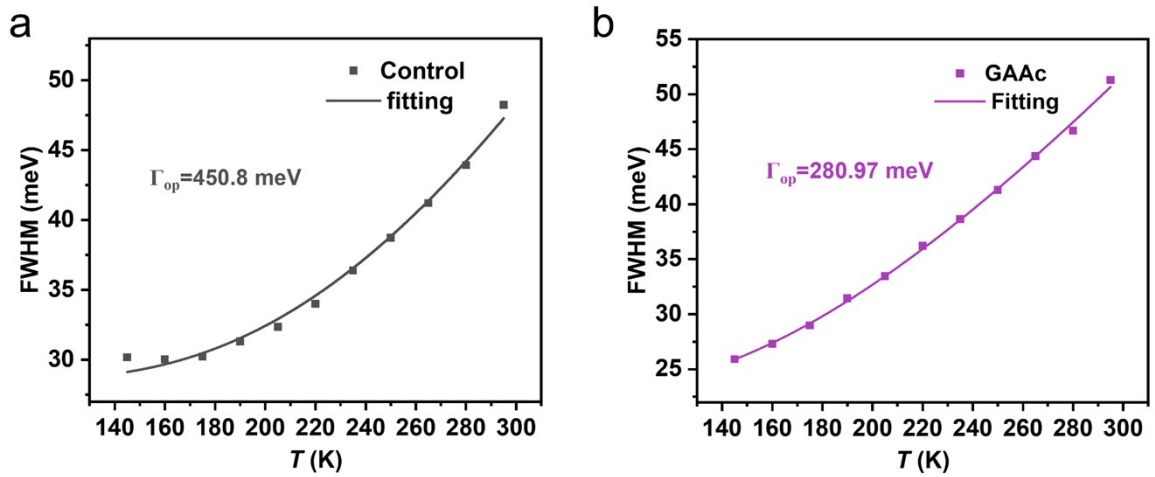

Fig. S13 The FWHMs of the (a) control and (b) GAAc treated perovskites as a function of temperature.

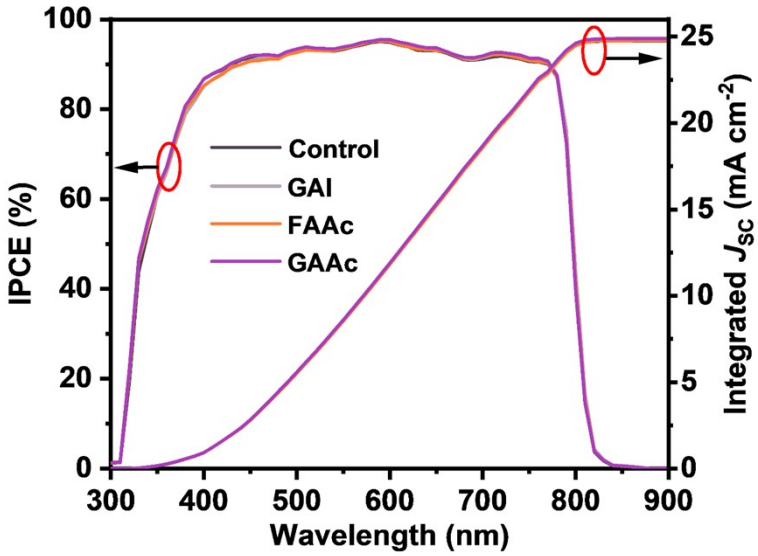

Fig. S14 EQE and integrated J_{SC} of the control, GAI, FAAc, and GAAc treated PSCs.

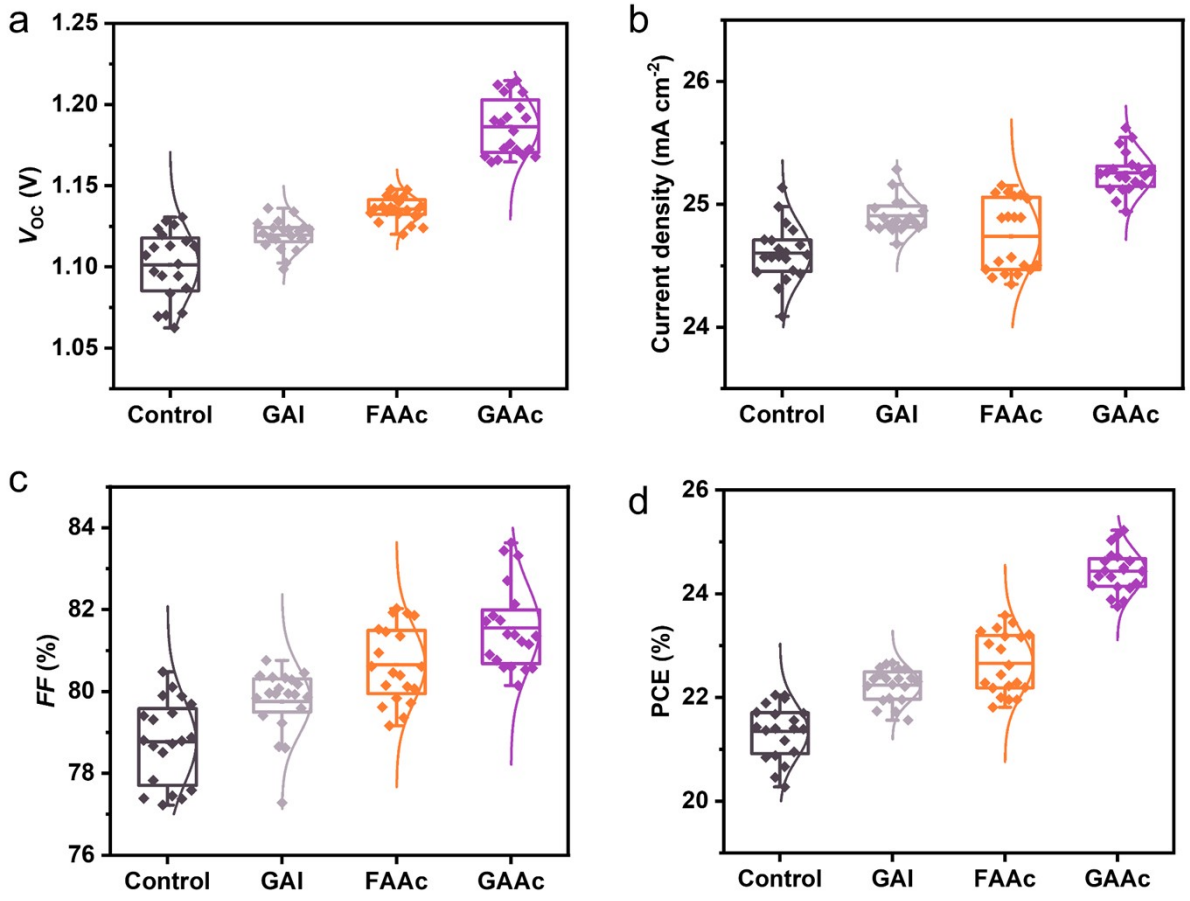

Fig. S15 Statistic diagram box of the photovoltaic parameters of the control, GAI, FAAc, and GAAc treated PSCs. (a) V_{OC}, (b) J_{SC}, (c) FF, and (d) PCE.

福建省计量科学研究院
FUJIAN METROLOGY INSTITUTE
（国家光伏产业计量测试中心）
National PV Industry Measurement and Testing Center

中国认可 国际互认 检测 TESTING CNAS L0131

检 测 报 告
Test Report

报告编号：22Q3-00044
Report No.

客户名称 Name of Customer	Zhanhua Wei Group, Huaqiao University
联络信息 Contact Information	No. 668 Jimei avenue, Xiamen 361021, Fujian Province. P. R. China
物品名称 Name of items	perovskite solar cell
型号/规格 Type /Specification	Pb-based perovskite solar cell
物品编号 Items No	ZW2022-2
制造厂商 Manufacturer	Zhanhua Wei Group, Huaqiao University
物品接收日期 Items Receipt Date	2022-03-01
检测日期 Test Date	2022-03-01

福建省计量科学研究院 盖章处 证书/报告专用章 3501020056403

批准人 Approved by 黎健生 黎健生
核验员 Checked by 何翔 何翔
检测员 Test by 陈彩云 陈彩云

发布日期 Date of Report 2022 年 Year 03 月 month 04 日 Day

扫一扫 查真伪

本院/本中心地址：福州市屏东路 9-3 号 Address：9-3 Pingdong Road,Fuzhou,China
电话：0591-87845050 Telephone
传真：0591-87808417 Fax
邮编：350003 Post Code
网址：www.fjjl.net Web Site
咨询电话：0591-87845050 Inquire line
投诉电话：0591-87823025 Complaint Tel

福建省计量科学研究院
FUJIAN METROLOGY INSTITUTE
（国家光伏产业计量测试中心）
National PV Industry Measurement and Testing Center

报告编号：22Q3-00044
Report No.

检测结果/说明：
Results of Test and additional explanation.

1 Standard Test Condition (STC)： Total Irradiance： 1000 W/m^2
Temperature： 25.0 ℃
Spectral Distribution： AM1.5G

2 Measurement Data and I-V/P-V Curves under STC

Forward Scan

I_{sc} (mA)	V_{oc} (V)	I_{MPP} (mA)	V_{MPP} (V)	P_{MPP} (mW)	FF (%)	η (%)
3.055	1.162	2.832	0.9909	2.806	79.04	23.46

Reverse Scan

I_{sc} (mA)	V_{oc} (V)	I_{MPP} (mA)	V_{MPP} (V)	P_{MPP} (mW)	FF (%)	η (%)
3.058	1.166	2.890	1.005	2.904	81.44	24.28

Mismatch factor: 1.004

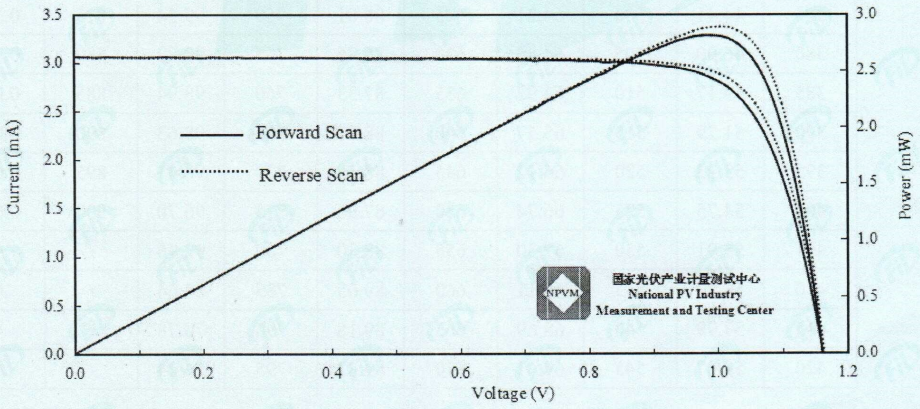

Figure 1. I-V and P-V characteristic curves of the measured sample under STC

检测报告续页专用
Continued page of test report

第 3 页/共 7 页
Page of Pages

Fig. S16 Certified efficiencies by FUJIAN METROLOGY INSTITUTE, National PV Industry Measurement and Testing Center.

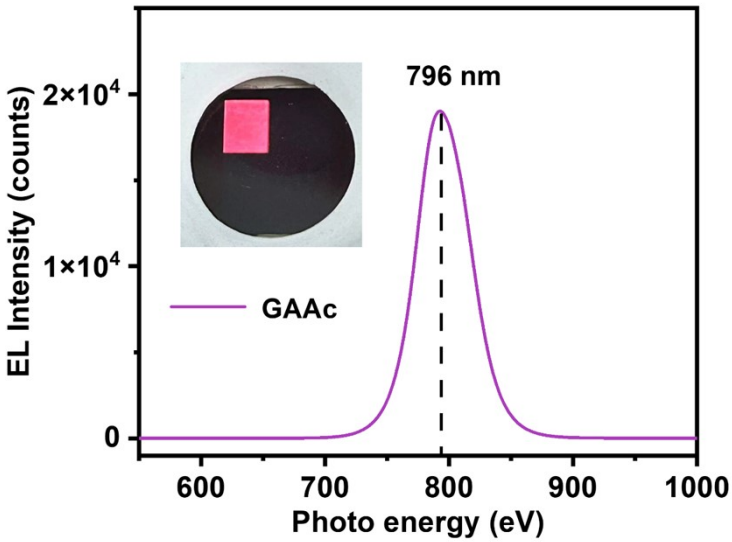

Fig. S17 EL spectrum of the GAAc treated PSC device work as an LED.

Table S1. Carrier lifetime of the control, GAI, FAAc and GAAc treated perovskite films.

Sample	τ_1(ns)	τ_2 (ns)	A_1	A_2	τ_{ave} (ns)
Control	228.90	972.19	583.27	307.43	742.69
GAI	253.94	1327.69	399.05	468.77	1177.34
FAAc	268.87	1600.73	444.03	469.39	1418.13
GAAc	285.27	2192.80	370.77	545.21	2037.76

Table S2. Integrated J_{SC} of the control, GAI, FAAc and GAAc treated PSCs.

Sample	Control	GAI	FAAc	GAAc
Integrated J_{SC} (mA cm^{-2})	24.76	24.88	24.78	24.91

Table S3. Detailed parameters for the hysteresis effect of the PSCs.

	V_{OC} (V)	FF (%)	J_{SC} (mA cm^{-2})	PCE (%)	Hysteresis (%)
$Control_{Forward}$	1.09	76.60	25.09	20.87	3.8
$Control_{Reverse}$	1.10	78.53	25.16	21.69	
$GAI_{Forward}$	1.11	78.61	25.02	21.84	3.0
$GAI_{Reverse}$	1.12	79.96	25.10	22.52	
$FAAc_{Forward}$	1.12	79.51	25.07	22.36	3.5
$FAAc_{Reverse}$	1.14	80.94	25.10	23.18	
$GAAc_{Forward}$	1.17	82.77	25.25	24.44	0.7
$GAAc_{Reverse}$	1.17	82.98	25.27	24.61	

Reference

1. T. S. Sherkar, C. Momblona, L. Gil-Escrig, J. Ávila, M. Sessolo, H. J. Bolink and L. J. A. Koster, *ACS Energy Letters*, 2017, **2**, 1214-1222.
2. T. Ding, R. Li, W. Kong, B. Zhang and H. Wu, *Applied Surface Science*, 2015, **357**, 1743-1746.
3. G. Kresse and J. Furthmüller, *Physical Review B*, 1996, **54**, 11169-11186.
4. M. Szafrański and A. Katrusiak, *Physical Review B*, 2000, **61**, 1026-1035.